Noise Induced Complexity: From Subthreshold Oscillations to Spiking in Coupled Excitable Systems

M. Zaks, X. Sailer, and L. Schimansky-Geier

Institut für Physik, Humboldt-Universität zu Berlin,

Newtonstr. 15, D-12489 Berlin, Germany

A. Neiman

Department of Physics and Astronomy,

Ohio University, Athens, OH 45701, USA

(Dated: February 2, 2008)

Abstract

We study stochastic dynamics of an ensemble of N globally coupled excitable elements. Each element is modeled by a FitzHugh-Nagumo oscillator and is disturbed by independent Gaussian noise. In simulations of the Langevin dynamics we characterize the collective behavior of the ensemble in terms of its mean field and show that with the increase of noise the mean field displays a transition from a steady equilibrium to global oscillations and then, for sufficiently large noise, back to another equilibrium. Diverse regimes of collective dynamics ranging from periodic subthreshold oscillations to large-amplitude oscillations and chaos are observed in the course of this transition. In order to understand details and mechanisms of noise-induced dynamics we consider a thermodynamic limit $N \to \infty$ of the ensemble, and derive the cumulant expansion describing temporal evolution of the mean field fluctuations. In the Gaussian approximation this allows us to perform the bifurcation analysis; its results are in good agreement with dynamical scenarios observed in the stochastic simulations of large ensembles.

PACS numbers: 05.40-a, 05.45.Xt

Recent studies have shown that noise may greatly enrich dynamics of nonlinear systems. This contradicts an intuitive conception on a simple blurring effect of noise added to a dynamical system. Thus, the quantitative measures of noise become additional control parameters of the system, extending its parameter space. For instance, variation of noise intensity may lead to qualitative transformations in the spatio-temporal dynamics. Thus noise changes the complexity of a system. As an example of such behavior we present an ensemble of globally coupled excitable elements. We let Gaussian white noise act additively and independently on each element of the ensemble. Simulations of the coupled Langevin equations as well as the bifurcation analysis of the equations for the lowest five cumulants show a rather complex sequence of qualitative changes when the intensity of the additive noise is varied.

I. INTRODUCTION

Noise-enhanced order in nonlinear dynamics far from equilibrium has become a rapidly growing area of modern statistical physics. Stochastic resonance [1], directed fluxes in stochastic ratchets [2], noise-induced phase transitions [3] are intensely discussed phenomena in nonlinear stochastic systems. Common to all of them is that an increase of the noise level results in a more ordered spatio–temporal response. This growth of order can be expressed and measured using various quantities. In particular, application of information theory allowed to quantify directly the noise-enhanced ordering and information transfer in bistable and excitable systems [4, 5, 6].

A broad class of dynamical systems with diverse applications is characterized by excitable dynamics. Chemical reactions [7], lasers [8], models of blood clotting [9], cardiac tissues [10] and nerve cells [11] belong to its most prevalent realizations. An excitable system possesses a stable equilibrium state (or rest state) from which it can temporarily depart if disturbed by a large enough stimulus: the system responds with a spike, a large excursion in its phase space, returning back to the rest state through a refractory period. Fundamental phenomena in excitable systems, such as pulse propagation, spiral waves, spatial and temporal chaos and synchronization are well studied [12, 13, 14, 15].

Analysis of the influence of noise on excitable dynamics has recently attracted great

attention [16, 17, 18, 19, 20, 21, 22, 23, 24, 25, 26, 27] as a necessary step towards realistic description of natural systems. The inclusion of fluctuations into models of excitability is desirable due to their omnipresence in processes of signal transmission and detection [28] which constitute often an interplay of signals and noise. Hence, the strength of variability as a measure of the present noise enters the excitable models as a *new* parameter [22]. That is why excitable dynamical systems *per se* are in nonequilibrium and the acting noise is unbalanced with respect to dissipative forces. Hence, a variation of noise often may induce qualitative changes in the performance and functioning of excitable systems which can be characterized in terms of the dynamics of moments and their bifurcations [29, 30, 31, 32, 33, 34].

A variety of models was proposed to describe different regimes of excitable systems, including dynamics of excitable, spiking, and bursting neurons [35]. Here we concentrate on one of the most popular systems, the FitzHugh-Nagumo model which was derived from the Hodgkin-Huxley model of the giant squid axon [13]. Despite its relative simplicity it displays a variety of biologically relevant dynamical regimes if taken as a single element or embedded into a network. It has been shown that the influence of noise on excitable systems such as the FitzHugh-Nagumo model can lead to a coherent temporal response via the phenomena of stochastic [1] and coherence [22, 36, 37] resonance.

In this paper we study noise-induced dynamics in a network of globally coupled FitzHugh-Nagumo elements, each with its own noise source. Most studies on noise-induced transitions considered so-called multiplicative or parametric noise or noise being colored [3]. In contrast, in our case excitable elements are driven by *additive* Gaussian *white* noise. Being statistically independent in different elements, noise sources possess the same intensity, T, which we use as a control parameter. We concentrate on the parameter region where a single uncoupled element possesses a stable equilibrium and is excitable. We simulate the stochastic equations and show that variation of T results in a rich variety of regimes of the collective response the ensemble, expressed in terms of the mean field (Section II). In order to delineate dynamical mechanisms behind these transitions we use cumulant approach in Gaussian approximation, thereby passing from a description in terms of coupled Langevin equations to a deterministic system of the fifth order for the cumulants of the ensemble distribution. This system is further analyzed by methods of the bifurcation theory (Section III). In particular, separation of timescales allows to identify the transition from irregular minor oscillations to regime of intermittent spikes of large amplitude as the canard explosion of a chaotic attractor. We

demonstrate that the spiking regime, whether regular or irregular, is possible: (a) only in the restricted interval of noise intensities, and (b) for moderate values of the coupling strength: a too strong coupling holds the ensemble together and keeps it close to the equilibrium; a too strong noise maintains the uniform distribution with non-oscillating mean values.

II. LANGEVIN APPROACH: NUMERICAL SIMULATION

As a prototype of an ensemble of excitable units we investigate the set of N noise-driven FitzHugh-Nagumo systems. The individual systems are coupled through the mean field and obey the equations:

$$\begin{aligned} \epsilon \dot{x}_i &= x_i - \frac{x_i^3}{3} - y_i + \gamma\,(\langle x\rangle - x_i), \\ \dot{y}_i &= x_i + a + \sqrt{2T}\,\xi_i(t), \qquad i = 1, \ldots, N. \end{aligned} \tag{1}$$

In the biochemical context the variables x_i denote e.g. the values of the membrane potential whereas y_i are responsible for the inhibitory action. Here $\xi_i(t)$ are the independent ($\langle \xi_i(t)\xi_j(t)\rangle = \delta_{ij}$) white Gaussian noise sources with vanishing average which individually act on the recovery variables $y_i(t)$. This could be interpreted, e.g., as a random opening of ion channels [38] which stochastically changes the conductivity of a membrane [39].

In the absence of noise ($T = 0$) the system (1) possesses a unique equilibrium state with $x_i = -a$ and $y_i = a^3/3 - a$. The equilibrium is stable for $a^2 > \max(1, 1-\gamma)$ and unstable otherwise. This follows from the characteristic equation which reads

$$\left(\lambda^2 - \frac{1-a^2}{\epsilon}\,\lambda + \frac{1}{\epsilon}\right)\left(\lambda^2 - \frac{1-a^2-\gamma}{\epsilon}\,\lambda + \frac{1}{\epsilon}\right)^{N-1} = 0$$

and means that positive coupling strength γ, whatever large it is, does not influence the stability of equilibrium.

As instantaneous global characteristics of the set of FitzHugh-Nagumo systems we consider the first moments of the distribution: mean field components $\langle x\rangle(t)$ and $\langle y\rangle(t)$.

The evolution equations (1) were solved numerically for the ensemble of $N = 10^5$ oscillators at different values of the noise intensity T. For our computations, we take $\epsilon = 0.01$, separating thereby the characteristic timescales of the variables. Further, we choose the value $a = 1.05$ under which an individual system is excitable: if initial perturbation exceeds a certain threshold value, the system "fires" i.e. displays a spike of large amplitude before

finally settling down to the steady state. Since $(1-a^2)^2 < 4\epsilon$, the leading eigenvalues, which characterize the perturbation decay in the immediate vicinity of the equilibrium, are complex.

We begin with the moderate value of the coupling strength $\gamma = 0.1$ and investigate the temporary patterns of the mean fields for different values of the noise intensity T.

As soon as the noisy perturbations are introduced, the individual elements, from time to time, are kicked across the excitation threshold and exhibit spikes. However, under sufficiently low values of T such irregular spikes are very seldom and do not contribute to the mean fields. Of course, since the noise is white, the nearly simultaneous "firing" of large subsets of elements should occur for arbitrarily small T, but such events appear to be extremely rare, and we never observed them within the integration intervals of $t \leq 10^3$.

As seen in Fig.1, at low noise intensities the mean field exhibits only minor excursions from some average value. For $\langle x \rangle$ the time average virtually does not decline from the equilibrium state $-a$ whereas the time average of $\langle y \rangle$ gets shifted. The amplitude of these excursions grows with the increase of T. Besides, qualitative changes occur: for very small T dynamics of the mean field is akin to a non-biased random walk (Fig.1(a)), at slightly larger values of T the motion gradually acquires the character of noisy rotation (Fig.1(b)), and still higher values of T yield phase portraits which are reminiscent of the spiral chaotic attractor (Fig.1(c)). In order to exclude the numerical artefacts and diminish the finite-size effects we performed several control runs with a much higher ($N = 3.2 \times 10^7$) number of coupled systems and obtained in the latter case the even more pronounced pattern of the multi-band chaotic attractor.

Starting from $T \approx 2.76 \times 10^{-4}$ we observe the qualitative transition: minor ("subthreshold") oscillations of the mean field are interrupted by large outbursts (spikes). This is a consequence of the collective phenomenon: for a large proportion of the individual units the firing events occur almost synchronously. Immediately beyond the threshold the spiking of the mean field is intermittent: the length of time intervals between the spikes is strongly varying (Fig.2a). With the increase of T the interspike intervals become shorter and more homogeneous (Fig.2b). The number of minor oscillations between two subsequent spikes steadily decreases (Fig.2c), proceeding from very large values (dozens in Fig.2a) to 2-3 in Fig.2c, and 1-2 in Fig.2d. Finally, such minor oscillations completely disappear and the mean field exhibits frequent non-interrupted spiking (Fig.2e). Hence variation of noise creates a

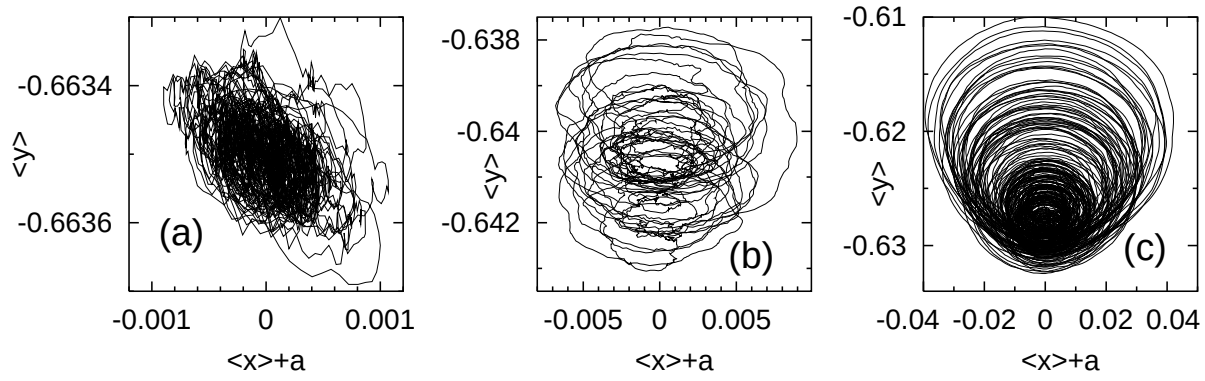

FIG. 1: Noise-induced onset of local oscillations around the equilibrium for $a = 1.05$, $\epsilon = 0.01$, $\gamma = 0.1$, $N = 10^5$: (a) $T = 10^{-4}$, (b) $T = 2.4 \times 10^{-4}$, (c) $T = 2.7 \times 10^{-4}$. Changes in the phase portrait indicate a bifurcation from disordered fluctuations to subthreshold oscillations. Note the smallness of the oscillation amplitude.

coherence resonance of the coupled ensemble.

The evolution of the phase portrait for the mean field is presented in Fig.3: the attractor which corresponds to the state of intermittent spiking consists of small and large loops (Fig.3a); the attractor of the non-interrupted spiking state is almost indistinguishable from the large-scale limit cycle (Fig.3b).

Noteworthy, transition to the spiking regime is accompanied by drastic changes in the power spectrum of the mean field. Just below this transition the spectrum possesses a well-defined peak which sits upon the noisy background and corresponds to the typical frequency of one minor rotation around the equilibrium (Fig.4a). Above the transition the mean field is characterized by the broadband spectrum (Fig.4b); the latter peak can still be vaguely identified, but there is no sharp contrast to the neighboring frequency values. A new feature of the power spectrum are the characteristic deep minima at the value which corresponds to the inverse "recovery time" as well as at its harmonics [40].

In fact, this minima, albeit not so pronounced, can be recognized already in Fig.4a. This is explained by the fact that the individual units of the ensemble exhibit intermittent spiking even before the transition of the mean field. Close before the threshold small clusters of such elements start to spike cooperatively, making thereby the inverse recovery time visible in the spectrum already at this stage.

The range of noise intensities which enable the regime of spiking is relatively narrow.

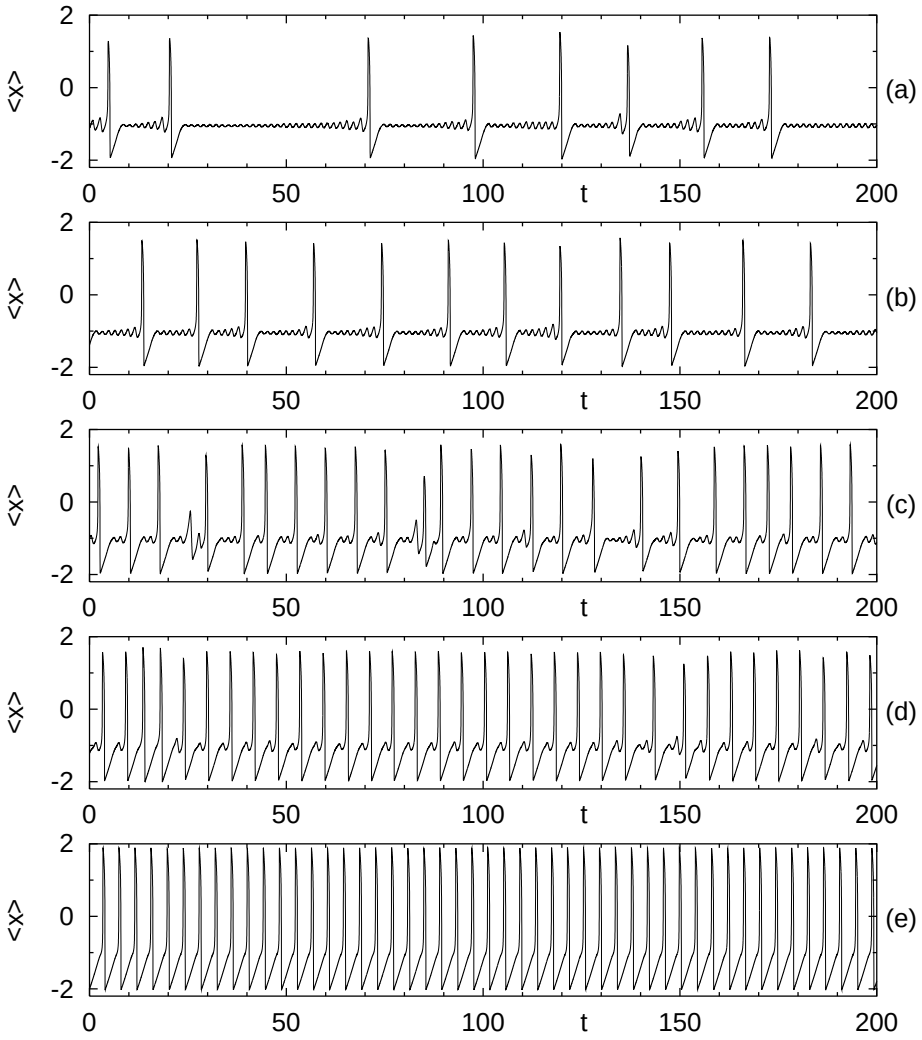

FIG. 2: Transition from intermittent spiking of the mean field to the regular spiking pattern. The sequence of pictures shows an increase of coherence in the response of the ensemble with respect to increasing noise. The noise intensity is varied: (a) $T = 2.77 \times 10^{-4}$, (b) $T = 2.8 \times 10^{-4}$, (c) $T = 2.9 \times 10^{-4}$, (d) $T = 3.0 \times 10^{-4}$, (e) $T = 3.1 \times 10^{-4}$, other parameters like in Fig. 1.

It is convenient to characterize the oscillatory states by means of the magnitude: distance between the global extrema of one of the mean fields, i.e. $d \equiv \max(\langle x \rangle) - \min(\langle x \rangle)$. In Fig.5a we present the dependence $d(T)$; it can be seen that after the initial abrupt growth the magnitude rapidly subsides. For the values of $T > 0.01$ no significant oscillations can be observed: mean fields $\langle x \rangle$ and $\langle y \rangle$ display only weak fluctuations around constant values. This indicates that the system has arrived at the steady distribution; however, in contrast to the sharp steady distribution at $T = 0$, in the latter case the width of the distribution

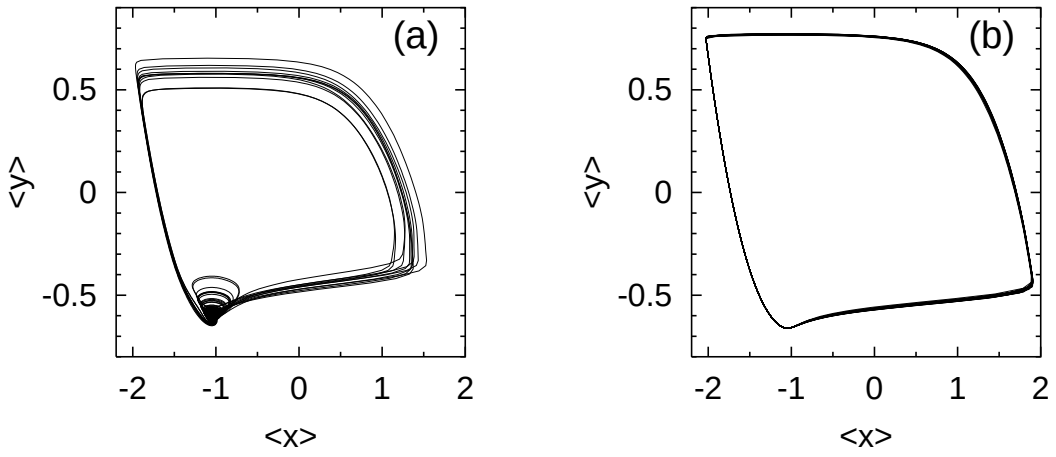

FIG. 3: Phase portraits of the mean field: (a) Intermittent spiking with $T = 2.77 \times 10^{-4}$, (b) Regular oscillations with $T = 3.1 \times 10^{-4}$, other parameters like in Fig. 1.

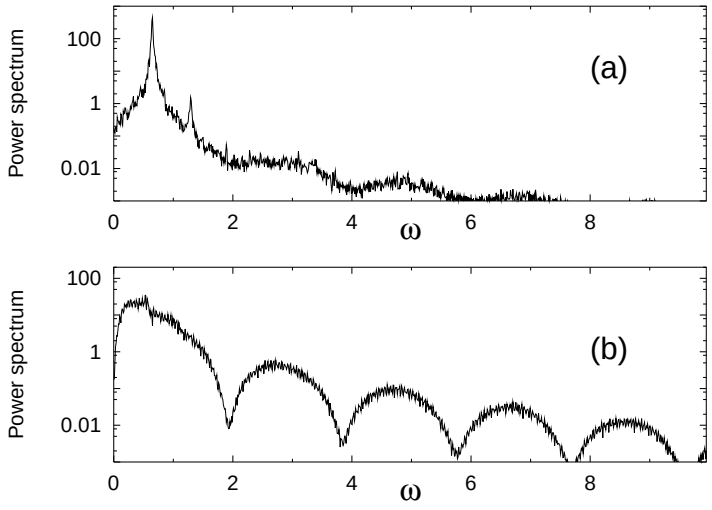

FIG. 4: Power spectra of the mean field $\langle x \rangle(t)$: (a) Regime of irregular subthreshold oscillations at $T = 2.73 \times 10^{-4}$, (b) Regime of intermittent spiking at $T = 2.76 \times 10^{-4}$, other parameters like in Fig.1. Minima in the spectral curve correspond to the inverse recovery time.

is quite large. Of course, the stationary distribution does not imply stationary states for individual units: since the noise intensity is high, each of them remains in the regime of frequent spiking. However, coherence between the individual spike events is lost, and the ensemble average displays no time dependency.

An increase of the coupling strength γ produces a quantitative change in this picture (Fig.5b): now the spiking state appears somewhat later and persists in a larger interval of

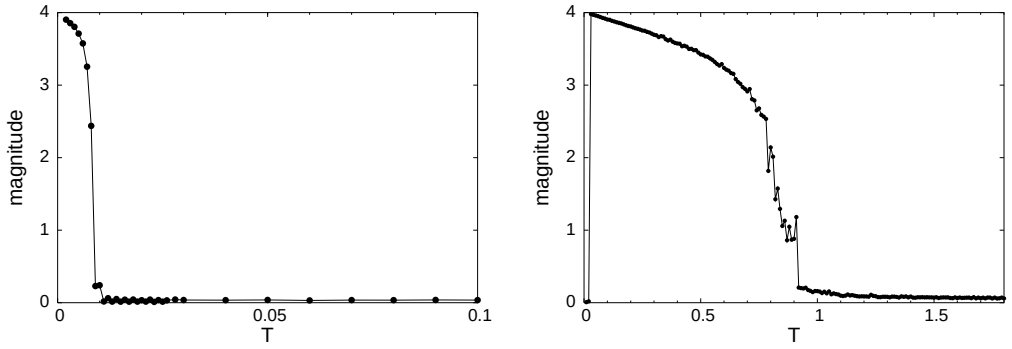

FIG. 5: Resonance-like dependence of the magnitude of oscillations on the noise intensity T for different coupling strength. Coupling enlarges the range of noise intensities where the resonance occurs. Left panel: γ=0.1; right panel: γ=1, other parameters like in Fig. 1.

the values of T. Qualitatively we observe the similar resonance-like picture with change of coupling strength: there exists a certain range of noise intensities which allows for the spiking regime of the mean field; both the too weak noise and the too strong one suppress the spiking. However, the enlargement of the noise range where spiking occurs proves that the array enhances the collective spiking.

The further growth of γ leads to disappearance of the spiking regime as well as of the state of minor oscillations: for $\gamma > 2.2$ we failed to observe significant temporal variations of the mean field at arbitrary noise intensities. Apparently, too strong coupling among the elements counteracts the noise: it holds individual systems together in the vicinity of the equilibrium and does not allow them to escape across the firing threshold[41].

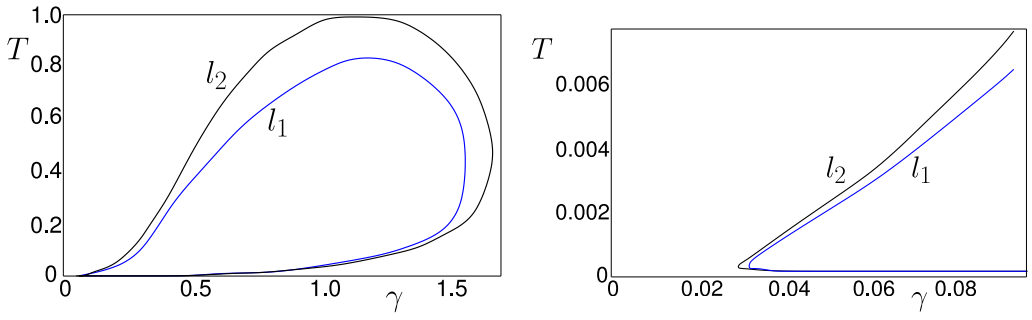

FIG. 6: Domains of existence of nonstationary regimes on the coupling-strength γ vs noise intensity T plane: there are no spiking states outside the inner curve l_1 and no oscillatory states at all outside the outer curve l_2. Left panel: global view; right panel: enlarged part for small values of γ, other parameters like in Fig. 1.

Boundaries of existence of nonstationary states on the parameter plane are shown in Fig.6. Here we see that not only the strong but also the weak coupling does not benefit the spiking state: apparently, for $\gamma < 0.03$ the coupling is insufficient in order to synchronize the firing events of individual elements. It should be noted that the upper part of the curve l_1 is somewhat ambiguous: here the spiking state arises from subthreshold oscillations in the course of decrease of T not via the abrupt transition, but rather through the continuous (although quite fast) growth of their amplitude; the plotted curve corresponds to the parameter values which ensure that the magnitude d equals 1.

Summarizing the results of numerical simulations, we state that the nonstationary mean fields can be observed only in a restricted range of the noise intensity, provided that the coupling strength does not exceed a certain value. Among those nonstationary states we can distinguish the chaotic subthreshold oscillations, the intermittent spiking regime and the regular spiking pattern.

III. GAUSSIAN APPROXIMATION: DYNAMICS OF CUMULANTS

A. Governing equations and geometry of phase space

The more detailed analysis of the set of coupled systems requires the deeper knowledge of the instantaneous distributions of x_i and y_i. In the limit of $N \to \infty$ such knowledge can be obtained from the analysis of the corresponding Fokker-Planck equation; presence of the coupling term in Eq.(1) adds to this equation the quadratic nonlinearity and destroys its variational character. Recently, the non-stationary Fokker-Planck equation for this problem was treated with the help of the expansion of the distribution density into the Hermite polynomials [26]; several interesting results were reported, but the global diagram of states is still missing.

Description in terms of the moments of distribution turns the problem into an infinite set of ordinary differential equations. In order to keep the problem tractable, one should either truncate the set of moments or come up with a plausible closure hypothesis. We choose the latter way and approximate the simultaneous state of the system by the Gaussian distribution of x_i and y_i with time-dependent parameters. Since for the Gaussian distribution (and *only* for it) all cumulants of the high order vanish, this assumption allows us to reduce

the infinite-dimensional problem to the low-dimensional model.

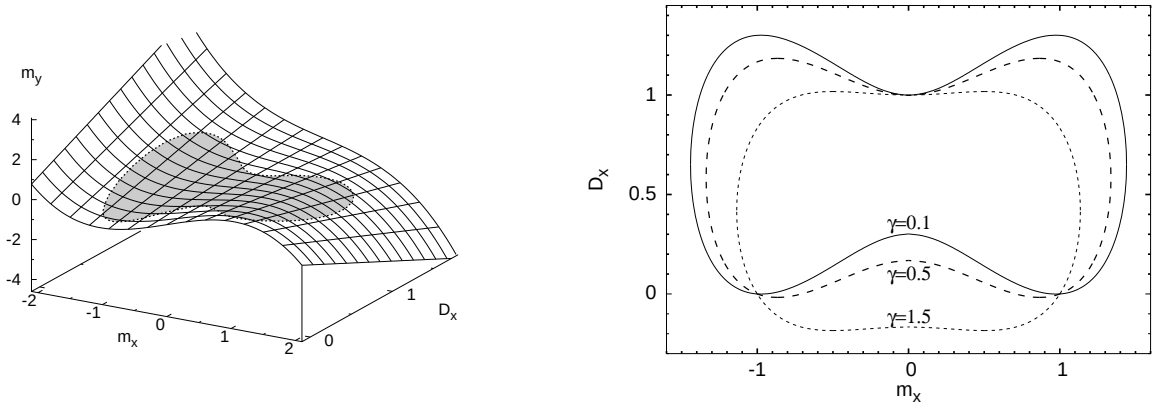

FIG. 7: a) 3-dimensional Projection of the twodimensional slow surface in the 5-dimensional phase space of the cumulant equations for $\gamma = 0.1$. Shaded domain: repelling region where inequality (5) holds. b) Repelling region on the slow surface for $\gamma = 0.1$, $\gamma = 0.5$ and $\gamma = 1.5$.

Let us average the evolution equations over the ensemble. Conditions of vanishing of cumulants of the 3rd and 4th order provide expressions for the higher-order moments $\langle x_i^3 \rangle$, $\langle x_i^2 y_i \rangle$ etc. On substituting these expressions into the averaged equations, we arrive at the dynamical system which governs the behavior of the cumulants $m_x = \langle x_i \rangle$, $m_y = \langle y_i \rangle$, $D_x = \langle (x_i - m_x)^2 \rangle$, $m_y = \langle (y_i - m_y)^2 \rangle$, $D_{xy} = \langle (x_i - m_x)(y_i - m_y) \rangle$ of the distribution:

$$\begin{aligned}
\epsilon \frac{d}{dt} m_x &= m_x - \frac{m_x^3}{3} - m_y - m_x D_x \\
\frac{d}{dt} m_y &= m_x + a \\
\epsilon \frac{d}{dt} D_x &= 2D_x(1 - D_x - m_x^2 - \gamma) - 2D_{xy} \\
\frac{d}{dt} D_y &= 2(D_{xy} + T) \\
\epsilon \frac{d}{dt} D_{xy} &= D_{xy}(1 - D_x - m_x^2 - \gamma) - D_y + \epsilon D_x
\end{aligned} \tag{2}$$

For small values of ϵ the separation of time scales in (2) turns m_x, D_x and D_{xy} into "fast" variables whereas m_y and D_y evolve on the slow time scale. Accordingly, in the 5-dimensional phase space there is a two-dimensional surface which corresponds to slow motions.

Location of this surface in the limit of vanishing ϵ is obtained by setting $\epsilon = 0$ in Eq.(2). It is convenient to parameterize the surface by coordinates m_x, D_x: given arbitrary values

of these two variables (of course, only non-negative values of D_x are physically meaningful) the three remaining coordinates are determined as

$$\begin{aligned} m_y &= m_x - m_x^3/3 - m_x D_x \\ D_{xy} &= D_x(1 - D_x - m_x^2 - \gamma) \\ D_y &= D_x(1 - D_x - m_x^2 - \gamma)^2 \end{aligned} \tag{3}$$

Solving the linear system

$$\begin{aligned} (1 - D_x - m_x^2)\,\dot{m}_x \quad & - m_x\,\dot{D}_x \quad = m_x + a \\ -(4m_x)\,D_x\,\dot{m}_x \;\; & +(1 - 3D_x - m_x^2 - \gamma)\dot{D}_x \;= D_x \;+\; \frac{T}{1 - D_x - m_x^2 - \gamma} \end{aligned} \tag{4}$$

for variables $\dot{m}_x$ and $\dot{D}_x$, yields evolution equations for dynamics *upon* the slow surface. [Explicit expressions are straightforward, but too long to be quoted here]. Stability of this surface with respect to *transversal* perturbations is governed by the sign of the determinant of the system (4): slow surface is repelling for

$$(m_x^2 - 1)^2 + D_x(3D_x - 4) < \gamma(1 - m_x^2 - D_x) \tag{5}$$

and attracting otherwise; notably, position and shape of the repelling region depend only on one of the parameters: the coupling strength γ.

One of the projections of the slow surface in the phase space is shown in Fig.7a; the butterfly-shaped repelling region is shaded. The geometry of the phase space has implications for the dynamics in general. We can expect that phase trajectories approach the attracting part of the slow surface and move along it; in case of penetrating into the region (5), they move for a certain time along the repelling surface (effect known as the "canard phenomenon"), depart from the slow surface and eventually approach the attracting part again.

Indeed, the bifurcation analysis of Eq.(2) discloses this picture.

B. From stationary distribution to small-scale chaos

We consider the equations (2) in the parameter range $a > 1$ where the solitary FitzHugh-Nagumo oscillator has a stable steady state. For $T \geq 0$ the equations (2) also possess the

unique steady solution in the domain $D_x, D_y \geq 0$:

$$\begin{aligned} m_x &= -a, \qquad D_x = \tfrac{1-a^2-\gamma+\sqrt{(1-a^2-\gamma)^2+4T}}{2} \quad , \\ m_y &= \frac{a^3}{3} - a + a\,D_x, \;\; D_y = \epsilon D_x + T(a^2 + D_x + \gamma - 1), \\ D_{xy} &= -T \end{aligned} \tag{6}$$

(there exists also the physically meaningless unstable state with negative D_x and D_y). This equilibrium describes the stationary distribution of oscillators; in the phase space the corresponding fixed point is located on the slow surface.

Destabilization of the equilibrium (6) under the increase of the noise intensity has a convenient graphical interpretation. Recall that shape and position of the repelling region on the slow surface depend only on γ. Fig.7b shows the outline of this region for several values of γ. As seen from Eq.(6), the equilibrium value of m_x is T-independent, whereas the value of D_x is the monotonically growing function of T. At T=0 the fixed point lies on the abscissa of Fig.7b. For all values of γ, the border of the repelling region passes through the point m_x=–1, D_y=0; part of the abscissa to the left from this point always lies in the attracting region. Accordingly, for $a > 1$ and arbitrary γ the stationary solution is stable in the absence of noise and (by continuity) at very small values of T.

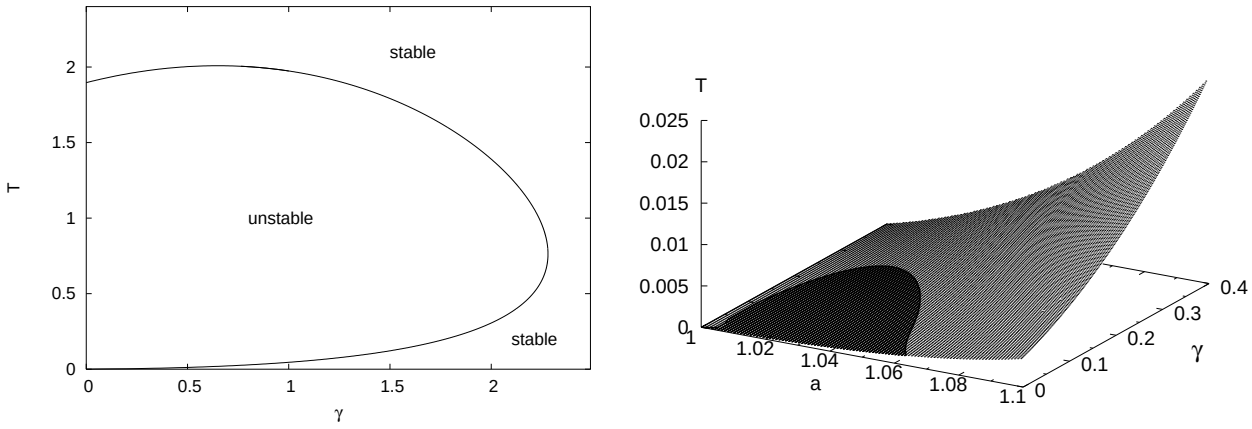

FIG. 8: (a) State diagram of the equilibrium at $a = 1.05$, $\epsilon = 0.01$. Region of stability is bounded by the curve of the Andronov-Hopf bifurcation. (b) Bifurcation surface of the Andronov-Hopf bifurcation in the parameter space of Eqs(2) with $\epsilon = 0.01$. The shaded region indicates a subcritical bifurcation.

As a consequence of the increase of T, the fixed point moves upwards along the vertical

line $m_x = -a$ and can cross the repelling region. Destabilization occurs when the fixed point hits the lower border of this region; in terms of Eqs (2) this event is the Andronov-Hopf bifurcation. In the limit $\epsilon \to 0$ the critical value T_H is given by the smaller root of the quadratic equation

$$9T^2 + T(16b^2 - 16 - 12b - 4\gamma + 9b\gamma + 2\gamma^2) + 2b(b+\gamma)^2(2 + 2b + \gamma) = 0 \qquad (7)$$

where $b \equiv a^2 - 1$.

To enable this instability, the vertical line $m_x = -a$ should cross the repelling region in Fig.7b. In terms of the parameter values this condition reads as

$$\gamma \leq \gamma_0 = 2(3a^2 - 1 - 2a\sqrt{3a^2 - 3}\,).$$

For $\gamma > \gamma_0$ the fixed point on the slow surface is always located to the left of the repelling region, and the equilibrium is stable for all values of T. This can be interpreted as stabilization of the equilibrium distribution by strong coupling. With the increase of a the value of γ_0 becomes smaller; it vanishes at $a = a_0 = \sqrt{1 + \sqrt{4/3}} \approx 1.467$. For $a > a_0$ the steady state is stable indendently of the values of γ and T. At small nonzero ϵ the qualitative and, largely, the quantitative picture persists; merely the values of γ_0 and a_0 slightly change.

Under sufficiently high values of T the fixed point moves over the upper border of the repelling region on the slow surface: the equilibrium regains stability. Again, this is the Andronov-Hopf bifurcation; the asymptotics at $\epsilon \to 0$ for the corresponding value of T is given by the larger root of Eq.(7). Shape of the bifurcation curve on the plane of parameters γ and T is shown in Fig.8a.

Thus we observe that in the domain of low and moderate values of γ the equilibrium exhibits two Andronov-Hopf bifurcations: the destabilizing and the stabilizing one. Computation of the cubic term in the amplitude expansion discloses a relatively small area on the parameter plane of a and γ where the first bifurcation is subcritical (Fig.8b): the unstable periodic solution branches off in the direction of small T. Here, a hysteresis occurs: the time-independent regime coexists with the stable oscillatory state; the latter is born from the tangent bifurcation shortly before the destabilization of the equilibrium. For most of the values of a and γ, however, the first Andronov-Hopf bifurcation is supercritical: the stable limit cycle with small amplitude $\sim \sqrt{T - T_H}$ and frequency $\sim \epsilon^{-1/2}$ is born. The second bifurcation is always supercritical: the stable limit cycle is born into the domain of

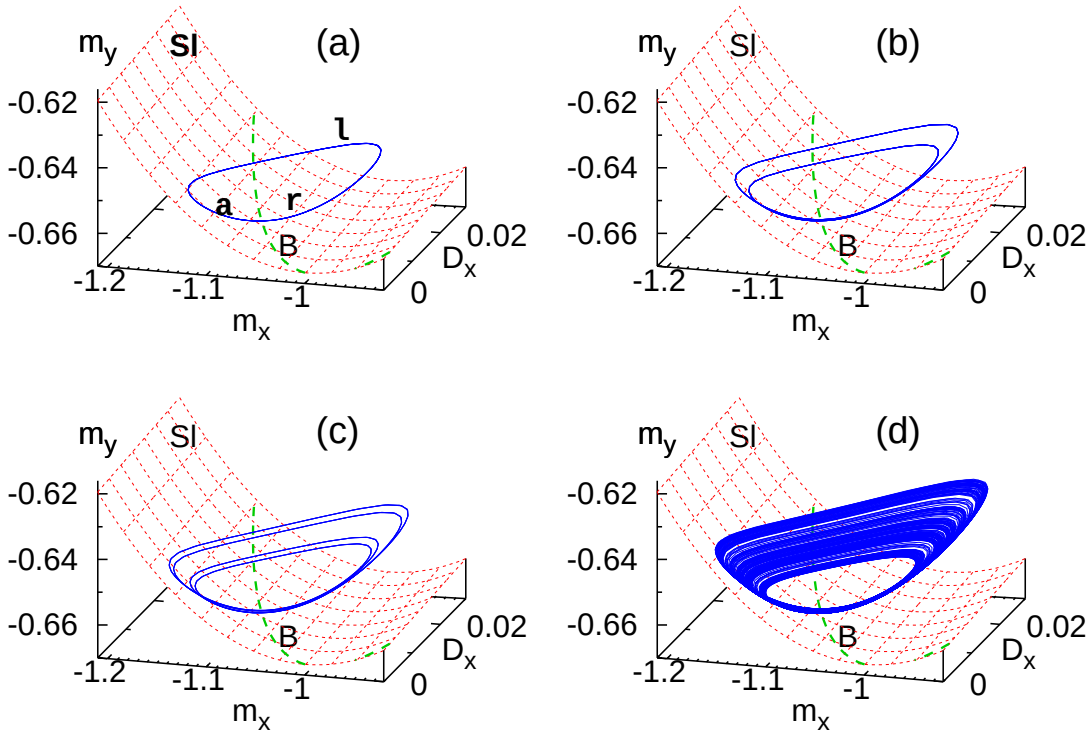

FIG. 9: Projections of phase portraits for Eqs(2) (cf. Fig. 7) for different regimes of local subthreshold oscillations. The dotted grid Sl shows the slow surface in the phase space. The surface Sl is stable to the left of the dashed line B. (a) $T = 0.00157$, (b) $T = 0.00158$, (c) $T = 0.0015826$, (d) $T = 0.001585$. Other parameters: $a = 1.05$, $\gamma = 0.1$, $\epsilon = 0.01$

lower values of T. With regards to finite-amplitude states, there seem to be no non-decaying solutions in the part of the parameter plane above the bifurcation curve in Fig.8a.

Near the lower branch of the bifurcation curve, the newborn limit cycle includes the segment (denoted by a in Fig.9a) which lies close to the attracting region of the slow surface, and the segment r which leads along the repelling region; from there, the orbit leaps back to the attracting region (segment l in Fig.9a).

Since the slow surface is two-dimensional, one can expect new qualitative effects in comparison to the single FitzHugh-Nagumo system with its S-shaped one-dimensional slow manifold. Indeed, when T is further increased, the periodic orbit loses stability by means of the period-doubling bifurcation. This event is followed by the sequence of further period-doublings which culminates in the onset of the chaotic state. In terms of the ensemble, the latter describes minor (localized) chaotic oscillations around the stationary distribution. Transformation of the attracting orbit and its position near the slow surface is depicted in

Fig.9;

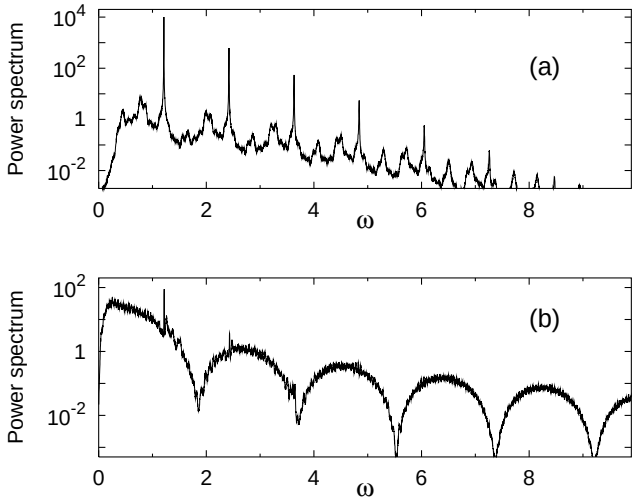

FIG. 10: Transition in the power spectrum of the cumulant equations. $a = 1.05$, $\gamma = 0.1$, $\epsilon = 0.01$. (a) T=0.001585, (b) T=0.001586.

The power spectrum of a trajectory on the chaotic attractor consists of the peak at the characteristic frequency of the minor oscillations, its harmonics and the broad noisy background (Fig.10a).

C. From chaotic to regular spiking

Further growth of T brings about dramatic changes in the shape and size of the attractor. As mentioned above, attracting orbits involve segments which lie close to the repelling part of the slow surface. In such situation a minute variation of the parameter may be a reason for the abrupt (albeit continuous) increase of the attractor size by several orders of magnitude: the so-called "canard explosion". This phenomenon has been well documented for the case when the attractor is a limit cycle (e.g. in the forced Van der Pol equation [42], and in the context of a single FitzHugh system disturbed by noise [43, 44, 45]). The peculiarity of our situation is that the "canard explosion" happens not to an individual periodic orbit but to the chaotic attractor as a whole (of course, individual unstable periodic orbits embedded into the attractor also experience the explosion, but this remains unnoticed for an observer who watches only the stable sets).

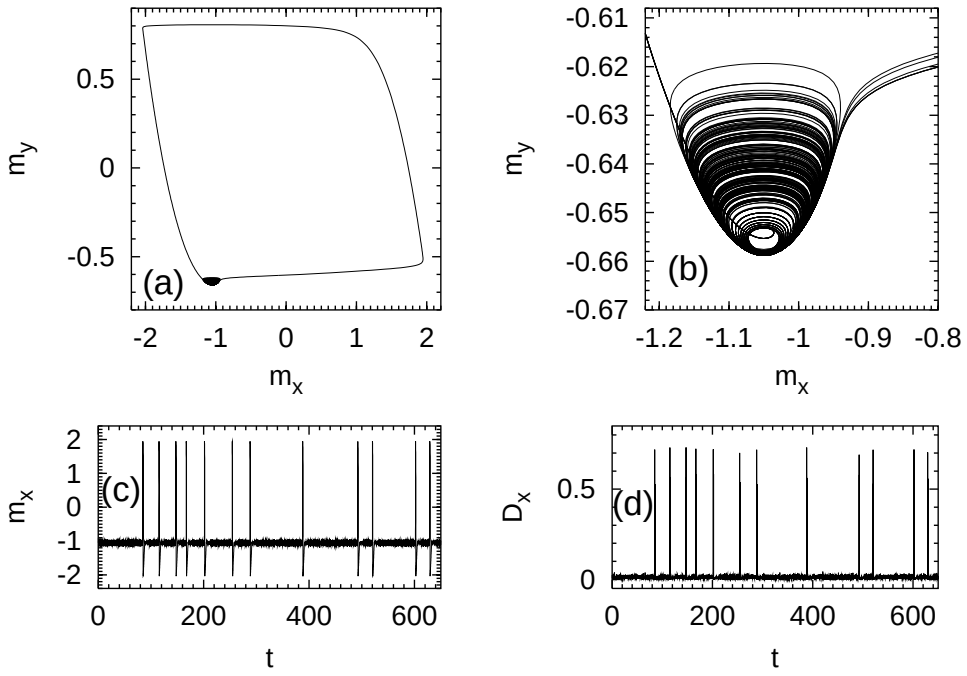

FIG. 11: Regime of irregular spiking in Eqs(2); a=1.05, γ=0.1, ϵ=0.01, T=0.001586. (a) projection of phase portrait; (b) enlarged part of phase portrait; (c) plot of $m_x(t)$; (d) plot of $D_x(t)$.

Projections of phase portraits and temporal evolution of the mean fields m_x and m_y in this state are shown in Fig.11. Apparently, this regime corresponds to intermittent chaotic spiking: after many minor oscillations in the vicinity of the unstable steady equilibrium, the system exhibits a spike of large amplitude, followed by the next epoch of localized chaotic oscillations.

A joint graphical presentation of the attractor and the slow surface is helpful for understanding the nature of spiking. The enlargement of the domain around the equilibrium in Fig.12a discloses that each arrival of a trajectory to this domain occurs via a steep descent into the "valley" along the slow surface. This return is followed by several minor revolutions, which share the familiar pattern: two segments along the, respectively, attracting and the repelling regions of the slow surface, and a return back to the attracting region. Finally, the trajectory "gets through" the slow surface [46] and is repelled far away from the equilibrium. A global picture (Fig.12b) indicates that this flight ends in the domain of positive m_x where the trajectory rapidly approaches the slow surface and moves along it for a certain time; the spike is accomplished by another fast flight back to the initial domain.

Accordingly, each single spike of the mean field is accompanied by two spikes of the

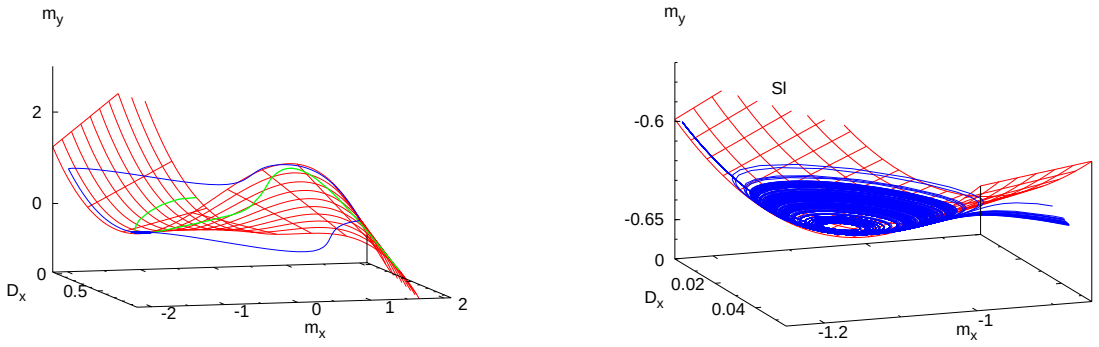

FIG. 12: Projection of the attractor and the slow surface in the state of irregular spiking. Left: global view of the attractor; right: enlargement of the domain near the unstable equilibrium.

variance (Fig. 13): the latter remains small on each of two slow segments but rapidly peaks during each of two fast flights.

Transition to the spiking regime is accompanied by sharp changes in the power spectrum of the process; this is shown in Fig.10b.

States with chaotic spiking occupy only a narrow strip in the parameter space. Further

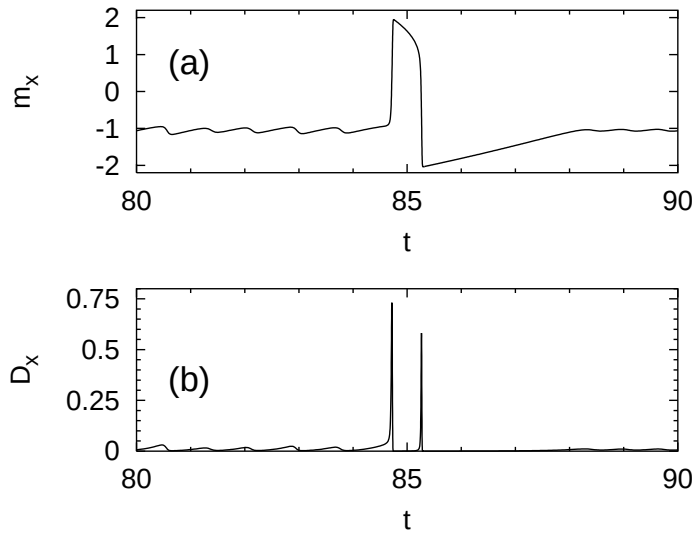

FIG. 13: Time evolution of the mean field and its variance within a single spike. (a) variable $m_x(t)$; (b) variable $D_x(t)$. Parameter values like in Fig.11. Rapid changes of m_x in either direction induce peaks of D_x.

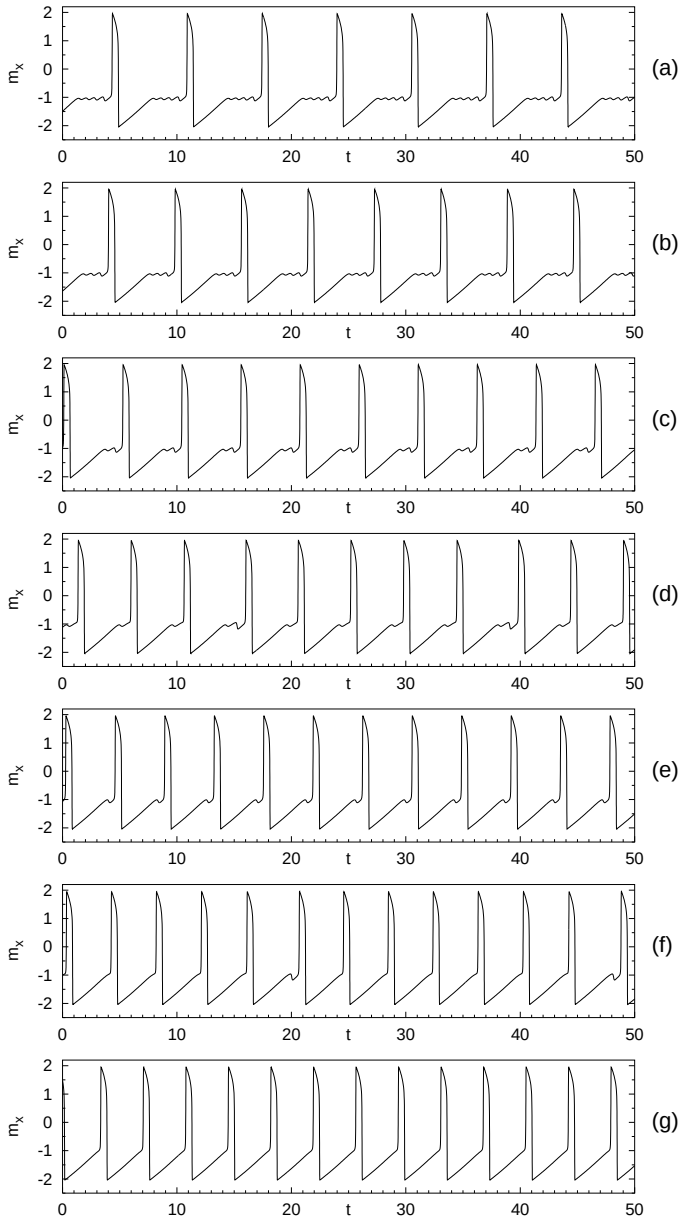

FIG. 14: Transition from intermittent to regular spiking in the cumulant equations with $\epsilon = 0.01$, $a = 1.05$, $\gamma = 0.1$: (a) $T = 0.00168$, (b) $T = 0.00172$, (c) $T = 0.00185$, (d) $T = 0.0018569$, (e) $T = 0.00220$, (f) $T = 0.0023105$, (g) $T = 0.0024$.

increase of T regularizes the spiking pattern: individual spikes are now separated by equal amounts of minor oscillations. With growth of T this amount gets smaller: it is a kind of the inverse "period-adding" sequence in which N localized oscillations between two subsequent spikes are replaced by N–1 ones (there is also a narrow transition region with more complicated states), then N–1 yields to N–2, etc [47]. Finally the minor oscillations com-

pletely disappear and the system proceeds into the regime of uninterrupted periodic spiking. Different stages of this process are shown in Fig.14 whereas the basic transition curves on the bifurcation diagram are plotted in Fig.15a.

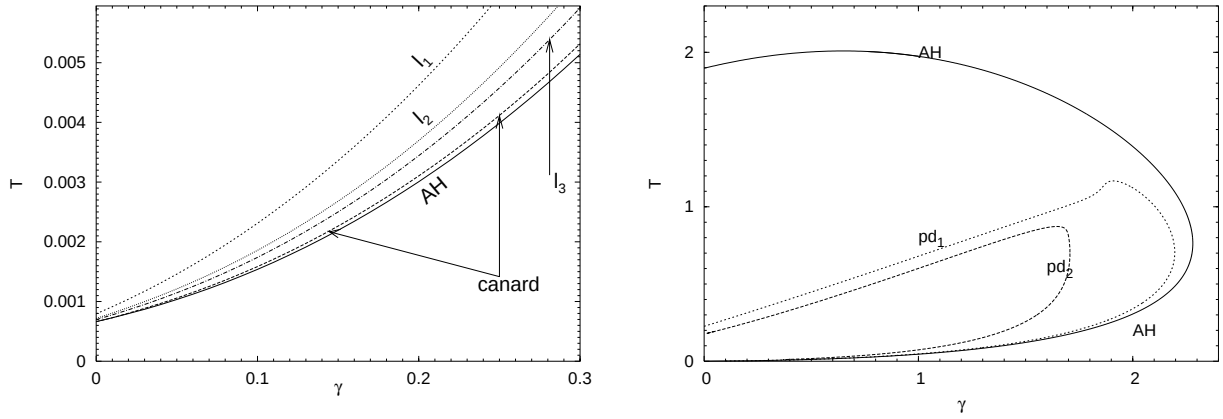

FIG. 15: a) Part of the bifurcation diagram for cumulant equations at $a = 1.05$, $\epsilon = 0.01$ for small values of the coupling γ. AH: Andronov-Hopf bifurcation; Canard explosion: onset of intermittent spiking oscillations, l_3: onset of regime with 2 minor oscillations between spikes, l_2: onset of regime with 1 minor oscillation between spikes, l_1: onset of regime without minor oscillation between spikes b) Important transitions on the parameter plane: AH: Andronov-Hopf bifurcation; $pd_{1,2}$: period-doubling bifurcations.

D. Strong noise: back from regular spiking to stationary state

As discussed above, under high values of T the only attractor of the system is the stationary state. Formally, it is the same solution (6) as in the case of low T; however, now this state describes the broad stationary distribution with high values of D_x and D_y. Here we briefly outline the way to this stationary state from the regular spiking pattern.

Quantitatively, we characterize the oscillations in terms of the same "magnitude" as in Sect.II: now this "attractor diameter" is defined as $d \equiv \max(m_x) - \min(m_x)$. Dependence of d on T for several fixed values of γ is shown in Fig.16.

We observe that the weak decay of the amplitude at low values of T is interrupted by the sharp decrease by a factor of ~ 2 which occurs within the narrow interval of T. This decrease is followed by the final interval of continuous decay until the periodic state disappears in

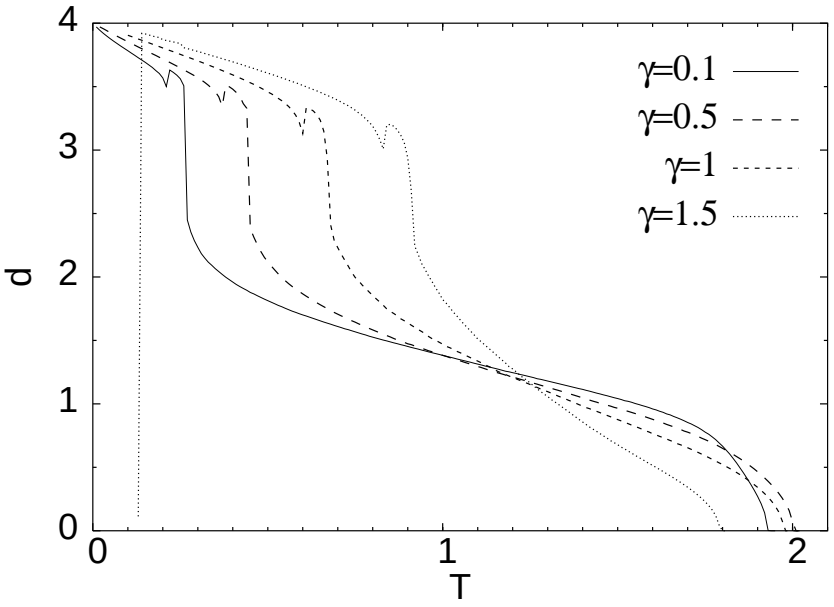

FIG. 16: Resonance like dependence of the magnitude of oscillations as function of the noise intensity T. Results of integration of the cumulant equations.

the Andronov-Hopf bifurcation; here, the segments of the curves obey the square-root law. The sharp decrease reminds of the canard explosion at low values of T, although it is less dramatic. At a closer look we see that the decrease is always preceded by a short interval in which $d(T)$ is non-monotonic. Checking the corresponding parameter values, we disclose here additional bifurcations. The local minimum of $d(T)$ corresponds to the period-doubling which occurs on the upper branch of the curve pd_2 on the parameter plane in Fig.15b.

This event is followed by the whole period-doubling scenario and the narrow range of T in which the spiking pattern turns chaotic again. In contrast to the previously described intermittent chaotic spiking, there are no small oscillations between the subsequent spikes; only the amplitudes of the spikes differ. The magnitude d weakly grows again, but in the course of the further minor increase of T the loops of the orbit "slide off" the broad part of the repelling region of the slow surface, and d rapidly decreases. Meanwhile, the chaotic state turns back into the regular one, and finally the reverse period-doubling bifurcation restores the simple periodic state. On the parameter plane the curve of the latter bifurcation turns out to be the upper branch of the already familiar period-doubling curve described in the previous subsection (line pd_1 in Fig. 15b). Fast "halving" of the attractor diameter takes place just below the curve pd_1; in the broad parameter range above this curve and below

the upper branch of the curve AH of the Andronov-Hopf bifurcation the amplitude of the limit cycle slowly decays.

For the values of γ to the left of the curve pd_2 ($1.7 < \gamma < 2.2$) the ordering of states is slightly different. Here the reverse period-adding sequence which simplifies the intermittent spiking pattern at low values of T, ends up in a limit cycle with several (4-6) spikes which exists over the broad range of T. Slightly below the upper branch of the curve pd_1 the transition to chaos occurs; it is followed by the reverse sequence of period-doubling bifurcations and very strong decrease of the diameter d.

Summarizing the results obtained from the analysis of the equations which govern the dynamics of the cumulants, we observe their remarkable qualitative correspondence with the basic knowledge obtained from the integration of the Langevin equations. Both the very weak and the very strong noise correspond to stationary probability distributions. Description in terms of the cumulants also confirms the stabilization of the stationary distribution by the strong coupling. The attractors of the cumulant equations practically do not differ from the phase portraits of the mean fields computed from simulations of the Langevin equations; the patterns of power spectra, especially for the state of intermittent spiking, also look strikingly similar. Besides, the analysis of the cumulant equations discloses the detailed picture of transitions between different non-stationary states: birth of the intermittent chaotic spiking from chaotic subthreshold oscillations and the subsequent regularization of the spiking pattern under the action of noise. Quantitatively, in the cumulant equations the critical values of the noise intensity which correspond to transitions between different states, turn out to be noticeably higher than those in the numerical simulations of large ensembles of FitzHugh-Nagumo systems.

IV. DISCUSSION AND CONCLUSIONS

We have investigated an ensemble of globally coupled FitzHugh-Nagumo elements under the action of additive Gaussian white noise. With the help of numerical simulations of stochastic equations we have verified that noise intensity becomes an additional control parameter of the system. By changing noise intensity we provoke qualitative transformations of the global response of the system, characterized by the mean field.

In order to gain better understanding of dynamical mechanisms of these transitions we

employed an approximate description in terms of cumulants of the Gaussian distribution. On the whole, modeling a large ensemble of globally coupled excitable units by the Gaussian distribution with time-dependent characteristics proved to be a fruitful approach: it has reduced the problem to the low-dimensional deterministic dynamical system which, in the large part of the parameter space, reproduced basic properties of the underlying stochastic ensemble. This allows us to conjecture that the fine details of the transitions between the states, accessible only in the framework of this model, keep relevance also for the whole ensemble.

In our example only the slow variables have been subjected to the additive noise. Of course, in the natural environment and in the laboratory experiments one cannot reduce the influence of fluctuations to only the slow variables: the fast ones can be affected as well. This can be accounted for, if the additive sources of Gaussian noise are included into the first of Eq.(1). We performed a set of numerical experiments with such equations, and observed, in general, the states similar to those described in the previous sections: steady distributions at high or very low noise intensities, subthreshold oscillations and spiking states in the intermediate range. The analysis of the respective cumulant equations can be pursued along the same lines as above. Since the noise acts on the fast variables, the shape and position of the repelling part of the slow surface depend now on the noise intensity; qualitatively, however, the only new effect in comparison with those described in Sect.III seems to be the direct transition from periodic subthreshold oscillations to regular spiking without the mediation of chaotic states; this is, of course, the usual canard explosion.

Of course, the Gaussian distribution is merely an approximation, and its applicability has certain restrictions. Thus, we failed to obtain the quantitative correspondence for small values of the coupling strength γ. Stochastic simulations indicate the absence of nonstationary regimes in this parameter range (cf. Fig.6b) whereas the analysis of the cumulant equations predicts the whole bifurcation scenario for arbitrarily low values of γ and even at $\gamma = 0$ (cf. Fig.15a). The higher the value of γ, the better the correspondence between the behavior of the stochastic equation (1) and the deterministic model (2). However, since the considered coupling is linear, an increase of its strength reduces the complexity of dynamics towards a linear system. Hence, under the strong coupling the Gaussian approximation becomes a more adequate model of the process, but the process itself gets simpler: there is little place for nonlinear events and, hence, variation of T fails to invoke transitions in the behavior of

the mean field.

Acknowledgement This work was supported by SFB-555, an international cooperation grant from the DAAD (D/0104610) and the NSF (INT-0128974).

---

[1] L. Gammaitoni, P. Hänggi, P. Jung, and F. Marchesoni, *Rev. Mod. Phys.* **70** (1998) 223.

[2] H. Linke (Editor), Appl. Phys. A **75** (2) (2002).

[3] J. Garcia-Ojalvo, and J. M. Sancho, *Noise in Spatially Extended Systems* (Springer-Verlag, New York, 1999).

[4] A. Neiman, B. Shulgin, V. Anishchenko, W. Ebeling, L. Schimansky-Geier and J. Freund, *Phys. Rev. Lett.* **76** (1996) 4299-4302.

[5] I. Goychuk, and P. Hänggi, *Phys. Rev. E* **61**, (2000) 4272-4280.

[6] I. Goychuk, *Phys. Rev. E* **64**, (2001) 021909.

[7] T. Sakurai, E. Mihaliuk, F. Chirila, and K. Showalter, *Science* **14** (2002) 296.

[8] H. J. Wünsche, O. Brox, M. Radziunas, and F. Henneberger, *Phys. Rev. Lett.* **88** (2001) 023901.

[9] E. S. Lobanova, E. E. Shnol, and F. I. Ataullakhanov, *Phys. Rev. E* **70** (2004) 032903.

[10] A. V. Panfilov, S. C. Müller, V. S. Zykov, and J. P. Keener, *Phys. Rev. E* **61** (2000) 4644.

[11] C. Koch, *Biophysics of Computation: Information Processing in Single Neurons*, (Oxford University Press, New York, 1999).

[12] J. D. Murray, *Mathematical Biology*, 2nd Ed. (Springer-Verlag, New York, 2003).

[13] A. S. Mikhailov, *Foundations of Synergetics I*, 2nd Ed. (Springer, Berlin-Heidelberg, New York 1994).

[14] T. R. Chay and J. Rinzel, *Biophysical Journal* **47** (1985) 357-366.

[15] B. Hu, and C. Zhou, *Phys. Rev. E* **63** (2001) 026201.

[16] S. Kádár, J. Wang, and K. Showalter, *Nature* **391** (1998) 770-772.

[17] P. Jung, A. Cornell-Bell, F. Moss, S. Kádár, J. Wang, and K. Showalter, *Chaos* **8** (1998) 567-575.

[18] A. Longtin, and D. R. Chialvo, *Phys. Rev. Lett.* **81** (1998) 4012.

[19] S. Bahar, A. Neiman, L A. Wilkens, and F. Moss, *Phys. Rev. E* **65** (2002) 050901(R).

[20] G. Schmid, I. Goychuk, and P. Hänggi, *Physica A* **325** (2003) 165 .

[21] G. Schmid, I. Goychuk, and P. Hänggi, *Physical Biology* **1** (2004) 61.

[22] B. Lindner, J. Garcia-Ojalvo, A. Neiman, and L. Schimansky-Geier, *Phys. Rep.* **392** (2004) 321.

[23] F. Liu, B. Hu, and W. Wang, *Phys. Rev. E* **63** (2001) 031907.

[24] C. Zhou, J. Kurths, and B. Hu, *Phys. Rev. E* **67** (2003) 030101(R).

[25] T. Kanamaru, T. Horita, and Y. Okabe, *Phys. Rev. E* **64** (2001) 031908.

[26] J. A. Acebron, A. R. Bulsara, and W.-J. Rappel, *Phys. Rev. E* **69** (2004) 026202.

[27] M. Schindler, P. Talkner, P. Hänggi, *Phys. Rev. Lett.* **93** (2004) 048102.

[28] H. Tuckwell, *Introduction to theoretical neurobiology*, (Cambridge University Press, 1988).

[29] A. N. Malakhov, *Radiofizika* **19** (1974) 71-81.

[30] R. Rodriguez, and H. Tuckwell, *Phys. Rev. E* **54** (1996) 5585.

[31] H. Hasegawa, *Phys. Rev. E* **68** (2003) 041909.

[32] S. Tanabe, and K. Pakdaman, *Phys. Rev. E* **63** (2001) 031911.

[33] R. Kawai, X. Sailer, L. Schimansky-Geier, and C. Van den Broeck, *Phys. Rev. E* **69** (2004) 051104.

[34] M. A. Zaks, A. B. Neiman, S. Feistel, and L. Schimansky-Geier, *Phys. Rev. E* **68** (2003) 066206.

[35] E. M. Izhikevich, *Int. J. of Bifurcation and Chaos* **10** (2000) 1171-1266.

[36] A. Pikovsky and J. Kurths, *Phys. Rev. Lett.* **78** (1997) 775.

[37] Y. Shinohara, T. Kanamaru, H. Suzuki, T. Horita, and K. Aihara, *Phys. Rev. E* **65** (2002) 051906.

[38] M. Falcke, *Adv. Phys.* **53** (2004) 255.

[39] We also performed simulations with noise terms in the activator equations, and obtained qualitatively similar results (see the concluding section).

[40] T. Prager, B. Naundorf, and L. Schimansky-Geier, *Physica A***325** (2003) 176.

[41] For the unbounded noise such rare large events should occur within sufficiently long time intervals, but such intervals by far exceed our numerical capabilities.

[42] P. Glendinning, *Stability, instability and chaos*, (Cambridge University Press, 1994).

[43] V. A. Makarov, V. I. Nekorkin, and M. G. Velarde, *Phys. Rev. Lett.* **86** (2001) 3431.

[44] E. I. Volkov, E. Ullner, A. A. Zaikin, and J. Kurths, *Phys. Rev. E* **68** (2003) 026214.

[45] F. Marino, G. Catalán, P. Sánchez, S. Balle and O. Piro, *Phys. Rev. Lett.* **92** (2004) 073901.

[46] Of course, this is only an optical illusion, a projection effect: a two-dimensional surface does not divide the 5-dimensional space.

[47] K. Kaneko, *Prog. Theor. Phys.* **69** (1983), 403.

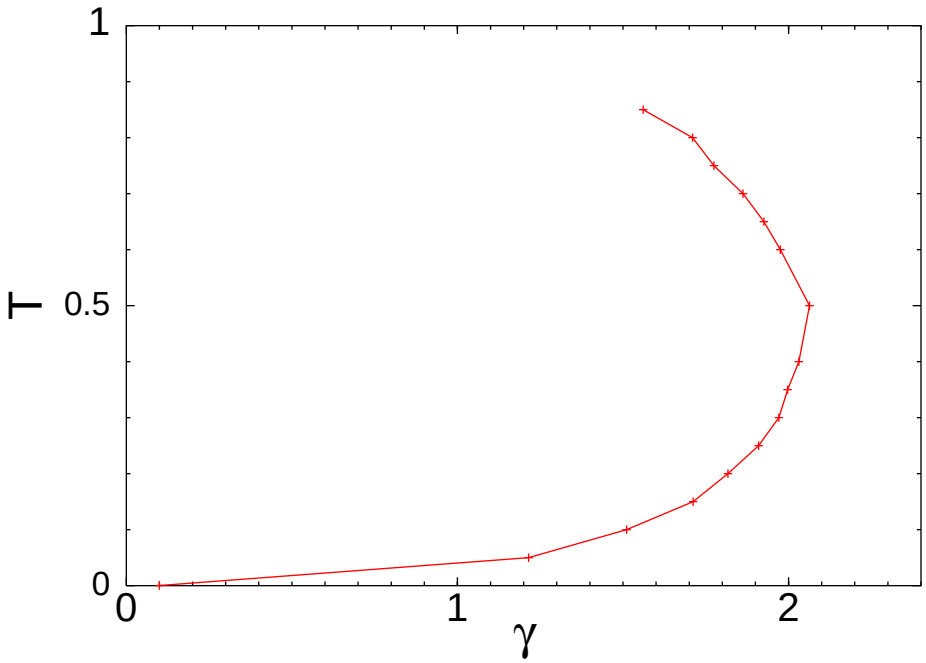
1
0.5
0
T
0
1
2
γ